Characteristic analysis of a novel F-P interferometer based on a pair of FBGs with built-in LPFGs*

WANG Chun-bao(王春宝), **ZHANG Wei-gang**(张伟刚)**, **RUAN Juan**(阮隽), **SHANG Jia-bin**(尚佳彬), **and YAN Ai-dong**(颜爱东)

Key Laboratory of Optoelectronic Information and Technology, Ministry of Education, Institute of Modern Optics, Nankai University, Tianjin 300071, China

(Received 26 November 2011)

The transmission characteristics of a Fabry-Pérot (F-P) interferometer based on a fiber Bragg grating (FBG) pair with a built-in long-period fiber grating (LPFG) are theoretically analyzed, and the shift of transmission interference fringe as a function of environmental refractive index is acquired. The influence of the lengths of F-P cavity, LPFG and FBG on the transmission characteristics of the proposed interferometer has been numerically investigated, and the simulation results indicate that the sensitivity of refractive index reaches 2.27×10^{-6} for an optical spectrum analyzer (OSA) with a resolution of 1 pm.

Document code: A **Article ID:** 1673-1905(2012)02-0084-5

DOI 10.1007/s11801-012-1039-x

Various applications of Fabry-Pérot (F-P) interferometers are found in many related areas. In the field of fiber sensing, fiber Bragg grating (FBG)-based F-P interferometers could be fabricated by inscribing two FBGs with the same parameters as reflectors[1], which could be utilized for detecting temperature and strain[2]. However, as fiber sensing systems are used for the measurement of environmental refractive index and absorption, the effective interaction between the light propagating in the fiber and the environmental media has been difficult. Many efforts have been put on the issue, including core mode leakage increased by etching fiber core or polishing fiber cladding[3,4], fiber cavity ring-down spectroscopy (CRDS) technique[5,6], filling materials in the air holes of photonic crystal fibers (PCFs)[7], mode coupling efficiency improvement via long-period fiber grating (LPFG)[8], etc.

Compared with FBGs with shorter grating periods, LPFG-based refractive index sensors have simple structure, avoiding polishing or etching the fiber cladding or filling materials in air holes of PCFs. However, the resonance bandwidth of LPFG is rather large, which will have influence on the refractive index sensing accuracy[9]. To solve the above issues, a novel FBG-based F-P interferometer with built-in LPFG has been investigated for high precision refractive index measurement[9].

By using transfer matrix method (TMM) to theoretically analyze the transmission characteristics of the FBG-based F-P interferometer with built-in LPFGs, we deduce the interference fringe shift as a function of environmental refractive index. Our theoretical analysis of the influence of interferometer parameters on its transmission characteristics would be of importance for the practical applications. Simulation results indicate that the refractive index sensitivity can reach 2.27×10^{-6} for an oscilloscope with a resolution of 1 pm.

The configuration of the proposed FBG-based F-P interferometer is shown in Fig.1. Two FBGs with the same low reflectance (FBG1 and FBG2) work as reflectors, and an LPFG pair is fabricated inside the F-P cavity. Part of the core-mode light can be coupled into fiber cladding modes in LPFG1, and later can be coupled again into the core mode in LPFG2. If the reflectivity of FBGs is high enough, and the reflection wavelength and resonance wavelength of the LPFG match well, the light in core mode within the FBG reflection bandwidth can be fully coupled into cladding modes. By measuring the interference fringe shift, the information on environmental refractive index can be acquired.

* This work has been supported by the National Natural Science Foundation of China (No.10974100), and the Tianjin Natural Science Foundation (No.10JCZDJC24300).

** E-mail:wangchunbao @mail.nankai.edu.cn

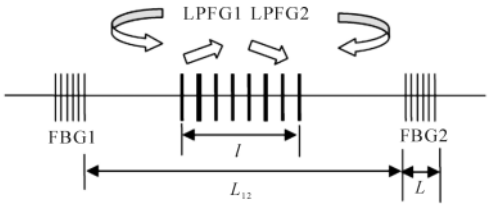

Fig.1 Schematic diagram of the F-P interferometer based on an FBG pair with built-in LPFG

The transmission characteristics of our proposed interferometer are determined by the FBGs and LPFGs employed in this structure. FBGs with uniform index modulation are analyzed by Rouard method[10] or mode-coupled theory[11].

For the F-P cavity consisting of two FBGs, the transmission function can be described as[11]:

$$T=\frac{(1-R_1)(1-R_2)}{\left(1-\sqrt{R_1R_2}\right)^2+4\sqrt{R_1R_2}\sin^2(\beta_{co}L_{12}+\frac{\varphi_1+\varphi_2}{2})}, \quad (1)$$

where R_1, $R_2=|\rho|^2$ represents the reflectivity for each grating, L_{12} is the spacing between two FBGs, β_{co} refers to the propagation constant of LP_{01} mode, and φ_1 and φ_2 are the reflectance phase of the two FBGs.

In the FBG-based F-P cavity, the light in core mode is coupled into cladding modes, and then re-coupled into core. The intracavity optical path is changed by the LPFG. According to LPFG theory[12,13], the initial amplitudes of co-propagating light in core mode and the *m*th cladding mode, namely $a_{co}(0)$ and $a_{cl,m}(0)$, respectively, after propagating through an LPFG with a length of *l*, can be described as:

$$a_{co}(l)=e^{i(\beta_{co}-\frac{1}{2}\Delta\beta^m)l}[a_{co}(0)(\cos sl+ i\frac{\Delta\beta^m}{2s}\sin sl)+a_{cl,m}(0)\frac{i\eta}{s}\sin sl], \quad (2)$$

$$a_{cl,m}(l)=e^{i(\beta_{cl,m}+\frac{1}{2}\Delta\beta^m)}[a_{co}(0)\frac{i\eta^*}{s}\sin sl+ a_{cl,m}(0)(\cos sl-i\frac{\Delta\beta^m}{2s}\sin sl)], \quad (3)$$

where

$$s=(\eta^*\eta+\frac{\Delta\beta^{m2}}{4})^{\frac{1}{2}}, \quad (4)$$

$$\Delta\beta^m=\beta_{co}-\beta_{cl,m}-\frac{2\pi}{\Lambda}, \quad (5)$$

where η is the LPFG coupling coefficient, Λ is grating period, and β_{co} and $\beta_{cl,m}$ represent the propagation constants of the core mode and the *m*th cladding mode, respectively. According to Eqs. (2)-(5), the phase variation induced by the LPFG inside the FBG-based interferometer could be described as

$$\delta=\frac{1}{2}(\beta_{co}+\beta_{cl,m})l+\pi. \quad (6)$$

From Eqs.(1) and (6), the transmission function of the FBG-based F-P interferometer can be expressed as

$$T'=\frac{(1-R_1)(1-R_2)}{\left(1-\sqrt{R_1R_2}\right)^2+4\sqrt{R_1R_2}\sin^2[\beta_{co}(L_{12}-l)+\frac{1}{2}(\beta_{co}+\beta_{cl,m})l+\pi+\frac{\varphi_1+\varphi_2}{2}]}. \quad (7)$$

From Eq.(7), it can be seen that the transmission spectrum has large peak value and narrow bandwidth if FBGs with weaker reflectivity are selected. Since the phase of LPFG is highly sensitive to environmental refractive index, i.e. $\beta_{cl,m}$ changes with environmental refractive index, the transmission interference fringe can shift accordingly. The resonance wavelength λ_{res} of an LPFG is determined by grating period Λ, and the effective refractive indices of the fiber core n_{co}^{eff} and cladding modes $n_{cl,m}^{eff}$. Then it is obtained as

$$\lambda_{res}=(n_{co}^{eff}-n_{cl,m}^{eff})\Lambda. \quad (8)$$

When the environmental refractive index changes, the relationship between resonance wavelength shift of LPFG and environmental refractive index is determined by[14]

$$\frac{d\lambda_{res}}{dn_{sur}}=\lambda_{res}\cdot\gamma\cdot\Gamma_{sur}, \quad (9)$$

where $\gamma=\frac{d\lambda_{res}/d\Lambda}{n_{co}^{eff}-n_{cl,m}^{eff}}$ is the waveguide dispersion factor, $\Gamma_{sur}=-\frac{\mu_m^2\lambda_{res}^3 n_{sur}}{8\pi r_{cl}^3(n_{co}^{eff}-n_{cl,m}^{eff})(n_{cl}^2-n_{sur}^2)^{3/2}}$ is the sensitivity factor, n_{sur} represents the environmental refractive index, n_{cl} is the refractive index of fiber cladding, r_{cl} refers to the cladding radius, and μ_m is the *m*th root of the first kind Bessel function.

When n_{sur} changes within 1.00−1.36, the LPFG resonance wavelength shift $\Delta\lambda_{res}$ can be regarded as varying linearly[14], i.e.

$$\Delta\lambda_{res}\approx\alpha_m\Delta n_{sur}, \quad (10)$$

where α_m is a parameter related to the resonance wavelength and mode order. From Eqs.(8) and (10), it could be seen that as the environmental refractive index changes, the effective refractive index of the *m*th cladding mode should be modified as

$$n_{cl,m}'^{eff}\approx n_{co,m}^{eff}-\frac{\alpha_m V n_{sur}}{\Lambda}. \quad (11)$$

According to Eq.(7), for maximum transmissivity, the intracavity phase should satisfy

$$2\beta_{co}(L_{12}-l)+(\beta_{co}+\beta_{cl,m})l+\varphi_1+\varphi_2=2N\pi \quad , \tag{12}$$

where N is an integer number. From Eqs.(11) and (12), we could obtain the interference fringe shift as

$$\Delta\lambda = \frac{\alpha_m \Delta n_{sur} l}{(2n_{co}^{eff} L_{12} - n_{co}^{eff} l + n_{cl,m}^{eff} l)\Lambda}\lambda_0 = \sigma \Delta n_{sur} \quad , \tag{13}$$

where λ_0 is the FBG resonance wavelength and σ represents shift coefficient.

According to Eq.(13), the relationship between shift coefficient and cavity length is shown in Fig.2. It is apparent that shift coefficient is highly sensitive to the cavity length in range of 10 − 60 mm, and the shorter cavity length, the larger shift coefficient. When cavity length is beyond 100 mm, it has little influence on shift coefficient. It can be seen that shift coefficient increases with the increase of LPFG length, which is further confirmed by Fig.3.

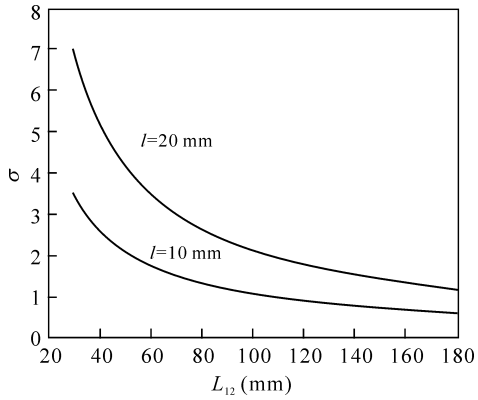

Fig.2 Shift coefficient as a function of F-P cavity length

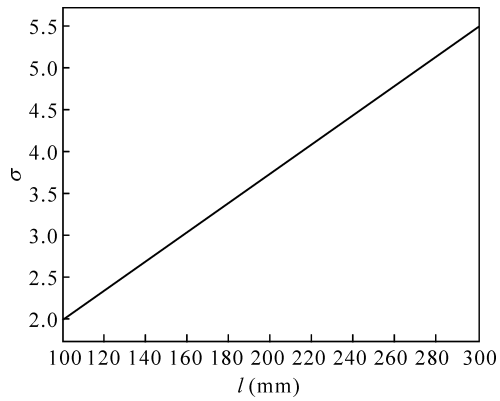

Fig.3 Shift coefficient as a function of LPFG length

The different dependences of wavelength shift on the lengths of LPFG (l) and F-P cavity (L_{12}) are shown in Fig.4 and Fig.5, respectively. Figs.4 and 5 indicate that there exists linear relationship between the wavelength shift and the environmental refractive index. From Figs.4 and 5, it is clear that the optimal shift coefficient can be acquired for the F-P cavity and LPFG lengths of 3−4 cm.

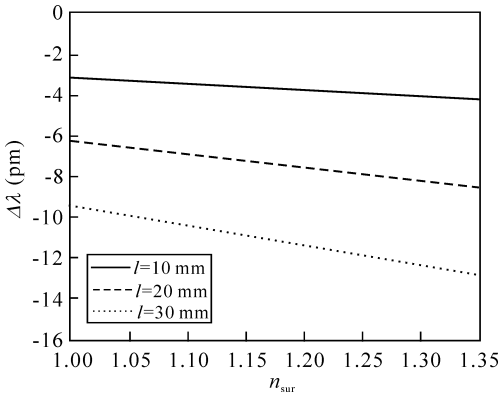

Fig.4 Wavelength shift as a function of environmental refractive index for different LPFG lengths

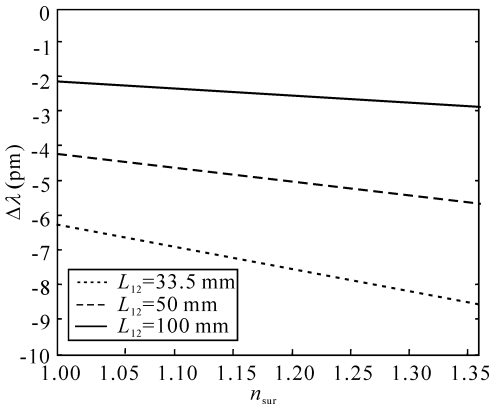

Fig.5 Wavelength shift as a function of environmental refractive index for different L-P cavity lengths

The B/Ge co-doped single-mode fiber[14] is adopted for our theoretical simulation. The specific fiber parameters are as follows: SiO_2 fiber material, B_2O_3 doping concentration of 9.7 m%, GeO_2 doping concentration of 4.03 m%, pure silica cladding, fiber radius of 3.8 μm, cladding radius of 62.5 μm, and core effective refractive index of 1.45. The period of FBG with the refractive index modulation of 5×10^{-5} is 524.8 nm, and its resonance wavelength is around 1522 nm. The period of LPFG with the refractive index modulation of 1.4×10^{-3} is 400 μm. According to Eq.(9), α_m is about 0.008 nm /10^{-3} for mode coupling between the core mode and the 6th cladding mode. According to Eq.(7), we can obtain the reflection spectrum of the interferometer.

From Fig.6, we could see that the reflection profile of the proposed interferometer is similar to that of a single grating. The number of transmission peaks increases with the increase of cavity length, and moreover the interference fringe becomes sharper with narrower free spectral range (FSR). The FSR of the transmission peaks in Fig.6 (a) is about 18 pm with a bandwidth of ~5 pm. It can be seen that sharp interference fringe can be ensured by employing FBGs as reflectors, and its reflectivity reaches 0.8 with narrow bandwidth

(determined by specific FBG parameters). Thus both of its reflection and transmission spectra can be utilized for measurement applications. However, since the bandwidth of transmission peak is narrower than that of the reflection peak, transmission spectrum would be more convenient for practical measurement.

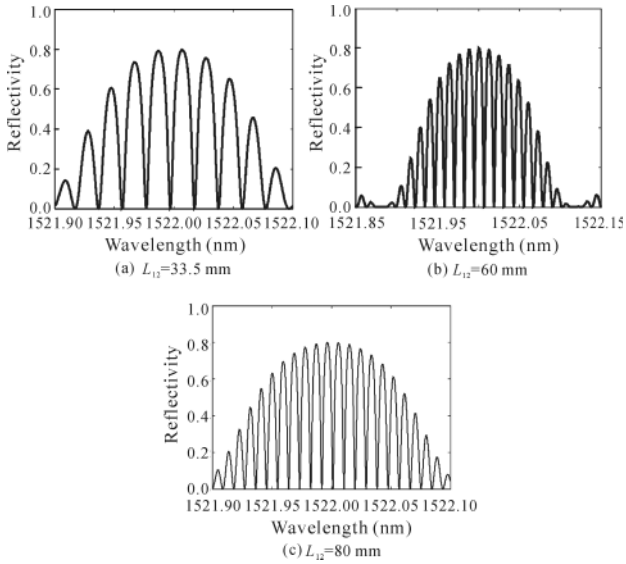

Fig.6 Interference spectra of the interferometer for different cavity lengths (*l*=28 mm,*L*=7 mm)

The length of the LPFG built in the FBG-based interferometer also has an impact on the interference spectrum. As shown in Fig.7, for fixed lengths of F-P cavity and FBG, the interference spectrum shifts toward shorter wavelength as the LPFG length increases. From Fig.7(b) and (c), the interference spectrum shifts toward shorter wavelength by about

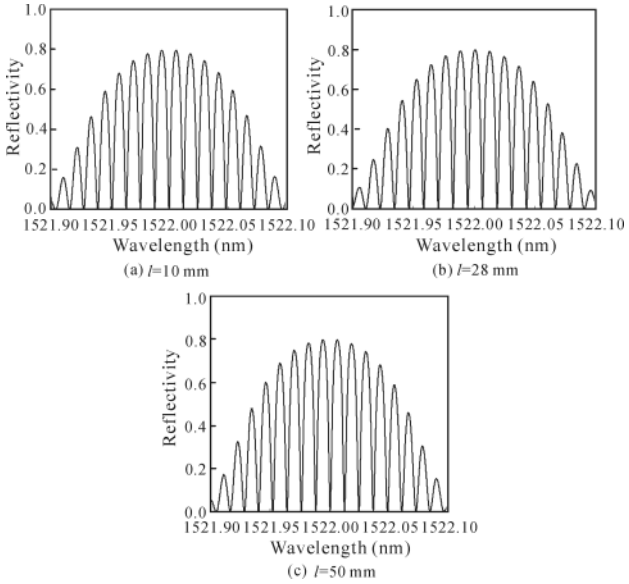

Fig.7 Interference spectra of the interferometer for different LPFG lengths (L_{12}=60 mm,*L*=7 mm)

6 pm. And for a certain reflection peak, the reflection peak value is also dependent on the spectrum envelope. Therefore, both of the interference fringe shift and the variation of reflection peak value should be considered in practical applications. Since the maximum transmission loss is 1, when transmission spectrum is exploited for measurement, only the fringe shift should be considered. The LPFG in F-P cavity not only alters intracavity phase but also excites the interaction between light in fiber core mode and environmental media. Hence longer LPFG should be selected with the prerequisite that the light in cladding mode coupled core mode could be re-coupled into core mode.

From Fig.8, it can be seen that with the increase of FBG length, the transmission value increases for interference peaks around the FBG resonance wavelength. As FBG length increases, the reflectivity of a single FBG increases, the bandwidth of resonance peak becomes narrower, and the reflectivity becomes lower for large detuning region. Since the interference envelope is dependent on the reflection spectrum of a single FBG, when FBG length increases, the reflectivity of large detuning region becomes higher. While with the increase of FBG length, the reflectivity for peaks around FBG resonance wavelength becomes higher, and the peak reflectivity of large detuning region becomes lower. The interference spectrum does not shift when FBG length changes. With the increase of FBG length, the bandwidth of transmission peaks becomes further narrower, and therefore sharper interference fringes may be obtained with high-reflectivity FBGs.

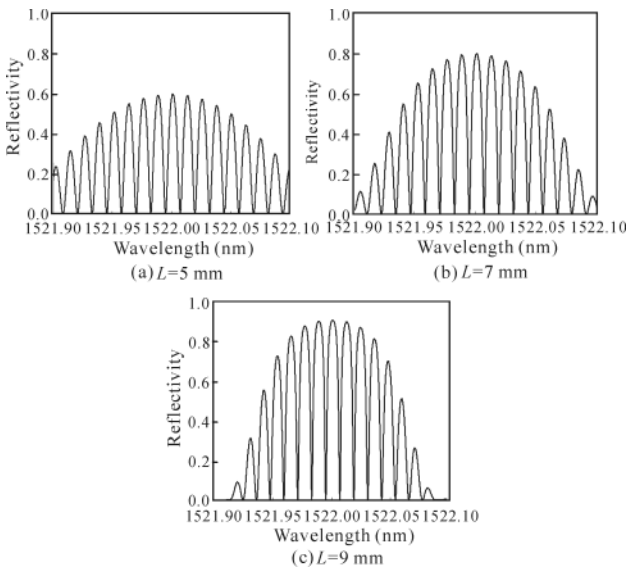

Fig.8 Interference spectra of the interferometer for different FBG lengths (L_{12}=60 mm,*l*=5 mm)

Besides, according to Eq.(13), for the environmental refractive index ranging from 1.00 to 1.36 and interferometer

setting of L_{12}=33.5 mm, l=28 mm and L=7 mm, the refractive index sensitivity can reach 2.27×10^{-6} when an OSA with a resolution of 1 pm is utilized.

The characteristics of an FBG-based F-P interferometer with built-in LPFGs are investigated in this paper. Theoretical analysis and numerical simulation indicate that sharp interference fringe with FSR of less than 20 pm can be achieved by employing FBGs as F-P cavity reflectors. The LPFGs inside the F-P cavity can adjust the intracavity optical path, and are highly sensitive to environmental parameters. The interference spectrum shift is theoretically modeled and deduced as a function of environmental refractive index. The influence of the lengths of F-P cavity, LPFG and FBG on the transmission spectrum is analyzed in detail. The proposed interferometer has several advantages, such as high sensitivity, simple structure and ease of application, and it could be utilized for high-sensitivity gas and liquid sensing applications. The research results in this paper provide a theoretical reference for the design and fabrication of FBG-based F-P interferometers.

References

[1] Guan Bai-ou, Yu You-long, Ge Chun-feng and Dong Xiao-yi, Acta Optica Sinica **20**, 34 (2000). (in Chinese)

[2] Zhuang Wang, Fabin Shen, Lijun Song, Xingwei Wang and Anbo Wang, IEEE Photonics Technology Letters **19**, 622 (2007).

[3] ZHAO Chun-liu, Journal of Optoelectronics • Laser **22**, 9 (2011). (in Chinese)

[4] XU Min, Zhu Tao, RAO Yunjiang, KE Tao and SHI Cui-hua, Journal of Optoelectronics • Laser **21**, 26 (2010). (in Chinese)

[5] LIU Bo, ZHANG Jian, LUO Jianhua, ZHANG Wei-hua, SHI Qing and KAI Gui-yun, Journal of Optoelectronics • Laser **18**, 1043 (2007). (in Chinese)

[6] Jiang Meng, Zhang Weigang, Zhang Qi, Liu Yaping and Liu Bo, Optics Communications **283**, 249 (2010).

[7] Zhang Weigang, Progress in Physics **27**, 449 (2007).

[8] Turan Erdogan, J. Opt. Soc. Am. A **14**, 1760 (1997).

[9] L. Mosquera, D. Sáez-Rodriguez, J. L. Cruz and M. V. Andrés, Optics Letters **35**, 613 (2010).

[10] Wang Chunbao, Zhang Weigang, Liu Zhuolin, Yan Aidong and Shang Jiabin, Chinese Journal of Lasers **37**, 1485 (2010).

[11] Yuri O. Barmenkov, Dobryna Zalvidea, Salvador Torres-Peiró, Jose L. Cruz and Miguel V. Andrés, Optics Express **14**, 6394 (2006).

[12] Han Y. G., Lee B. H., Han W. T., Paek U. C. and Chung Y., IEICE Trans. Electron. **E84-C5**, 610 (2001).

[13] Lee B. H., Kim Y. J., Chung Y., Han W. T. and Paek U.C., IEICE Trans. Electron. **E84-C5**, 621 (2001).

[14] Xuewen Shu, Lin Zhang and Ian Bennion, Journal of Lightwave Technology **20**, 255 (2002).